Picosecond Time-Resolved Study of 4-Dimethylaminobenzonitrile in Polar and Nonpolar Solvents

W. M. Kwok, C. Ma, and D. Phillips

Department of Chemistry, Imperial College, London SW7 2AY, U.K.

P. Matousek, A. W. Parker,* and M. Towrie

CLRC Rutherford Appleton Laboratory, Didcot, Oxfordshire OX11 0QX, U.K.

Received: August 5, 1999; In Final Form: February 15, 2000

By applying a Kerr gate to reject fluorescence, the picosecond time-resolved resonance Raman (TR^3) spectrum of the intramolecular charge-transfer (ICT) state of 4-dimethylaminobenzonitrile (DMABN) in a polar solvent has been obtained for the first time. To elucidate the geometric and electronic structural changes occurring in DMABN in different solvent environments following electronic excitation, the same method (without the Kerr gate) was also used to study the delocalized excited (DE) state of DMABN. The TR^3 spectrum of the ICT state is dominated by a phenyl ring band, while the band corresponding to the C≡N stretching mode is absent. The TR^3 spectrum of the DE state, observed in nonpolar solvents, implies a planar structure with double bond character in the $C_{ring}-N(CH_3)_2$ bond. Conjugation therefore extends mainly between the dimethylamino group and the ring in the DE state. The Kerr gate has also been used to measure the temporal spectral profile of the DMABN fluorescence in both nonpolar and polar solutions with 3 ps time resolution covering the spectral window from 320 to 560 nm. Subpicosecond transient absorption spectra of DMABN in solvents of different polarity have also been measured. The presence of an isosbestic point in the time-resolved fluorescence spectra at early time delays demonstrates the interchange of a two-state system during the initial relaxation process following the photoexcitation. The results are discussed and placed in context with the wealth of work performed to date on this molecular system.

1. Introduction

The dual luminescence of 4-dimethylaminobenzonitrile (DMABN) in a polar solvent was discovered by Lippert et al. in 1959.[1] Since then a great deal of effort has been devoted to determining the origin of this anomalous fluorescence behavior, and both steady-state fluorescence[2−4] and time-dependence fluorescence[5−7] measurements have been made. The main observations have been that in nonpolar solvents, such as alkanes with small polarizabilities, DMABN exhibits a single normal fluorescence band centered at ∼350 nm, historically termed the F_b band or "b-band", while in polar solvents a deeply red-shifted fluorescence band centered at ∼420−500 nm, termed the F_a band or "a-band", appears together with the F_b band. The F_b band emission is attributed to a less polar delocalized excited (DE) state, in earlier literature termed the locally excited (LE) state (because it is observed only in nonpolarizable solvents[8,9]), B* state, or ^1L_b-type (according to Platt's notation)[10] state. The frequency and intensity of the F_a band are solvent polarity dependent, which indicates the charge-transfer character and high polarity of this emitting state. Therefore, the F_a band was assigned to emission from a more polar intramolecular charge-transfer (ICT) state, A* state, or ^1L_a-type state. The polarities of the DE and ICT states have been confirmed by dipole moment measurements.[11,12] The red-shifted emission has also been found for many derivatives of DMABN and numerous electron donor−acceptor molecules where the two moieties are linked by a flexible single bond.[13−15]

A large number of different mechanisms have been proposed to account for the dual fluorescence of DMABN. The original model of Lippert et al.[16] suggests that the two bands correspond to emission from two different low-lying excited singlet states which invert in polar solvent. On the basis of different experimental observations, several alternative models have been introduced, such as the excimer model by Khalil et al.,[4] the excited state isomerization model by Grabowski et al.,[17,18] the proton-transfer model by Kosower et al.,[19] and the exciplex and complex model by Nakashima et al.,[20] Varma et al.,[21,22] and Eisenthal et al.[6] Recently, Zachariasse et al.[7,23,24] put forward a solvent-induced Jahn−Teller coupling model as the origin for the anomalous fluorescence. Of these models, the most widely accepted is the excited-state isomerization model, known as the TICT (twisted intramolecular charge transfer) model. According to this model,[17,18] DMABN dual fluorescence originates from two excited-state isomers differing in the orientation of the dimethylamino group relative to the aromatic ring. The F_b band emission arises from a planar isomer with the dimethylamino group situated in the plane of the ring. Charge is supposed to be distributed over the entire conjugated system and the dipole moment of this state is considered to be similar to that of the ground state. By contrast, the F_a band arises from a highly polar excited-state isomer, which is formed by twisting the dimethylamino group perpendicular to the plane of the ring, accompanied by a full intramolecular charge transfer from the lone pair on the amino N atom to the in-plane π^* orbital on the cyano group. The 90° twisted conformation leads to a practically complete electronic decoupling and complete loss of conjugation between the dimethylamino and benzonitrile groups (the principle of minimum overlap).[25] This electronic decoupling is thought to

10.1021/jp9927606 CCC: $19.00
Published on Web 04/15/2000

be necessary for prohibiting electron transfer in the reverse direction. The rotation of the dimethylamino group around the $C_{ring}-N(CH_3)_2$ bond was proposed to lower the energy of the highly polar state, which depopulates to the electronic ground state by emission of red-shifted fluorescence (the F_a band). In the TICT model, the presence of high polarity or polarizable solvent was thought to be necessary to yield the F_a emission. The decisive role of solvent polarity was referred to as solvent-induced $^1L_a-^1L_b$ level crossing and deemed necessary to stabilize the highly polar ICT isomer through mainly electrostatic interaction.[26−28]

The TICT model is supported by a considerable amount of experimental data. The best evidence comes from the comparison of a series of DMABN derivatives, from which only those with a rotatable dialkylamino group exhibit dual fluorescence in moderately polar solvents.[13,17] However, derivatives with the amino group forced into the ring plane by incorporation into a five- or six-membered ring exhibit only F_b emission.[13] On the other hand, compounds with steric hindrance to planarity such as 6-cyanobenzquinuclidine (CBQ)[29] or *N*,*N*-3,5-tetramethylaminobenzonitrile (TMABN)[13,30] yield only F_a emission, independent of the solvent polarity. However, Khalil et al.[31] have pointed out that the F_a emission behavior of CBQ and TMABN cannot be explained exclusively by the TICT model, because the observations merely indicate that the geometry restrictions on the ground state strongly affect the emissive behavior of the excited state. On the other hand, the large dipole moment measured for the ICT state,[11,12] the observation of a benzonitrile anion-like species in picosecond TA spectroscopy of DMABN in polar solvent,[32−34] and many theoretical studies[9,35,36] support the TICT model.

Further investigations on DMABN by various methods provide some challenges to the TICT model. Remaining unresolved questions about the TICT model can be summarized as the following:

(1) Is the structure of the ICT state twisted? If so, is it fully twisted? According to the solvent-induced Jahn−Teller coupling model proposed by Zachariasse et al.[7,23,24] for DMABN, the dimethylamino group N-inversion (wagging) is the most important reaction coordinate in the ICT process; the perpendicular twist of the amino group is thought not to be essential for the ICT state formation. It was suggested that the wagging motion of the amino group also decouples the donor from the acceptor orbitals, leading to formation of the ICT state with a greater dipole moment than the DE state.[7,11,24,37,38] Two mechanisms explaining the formation of the ICT state in terms of wagging motion have been proposed: the WICT (wagged intramolecular charge transfer) model suggested by Schuddeboom et al.[11,38] and the PICT (planar intramolecular charge transfer) model recently suggested by Zachariasse et al.[24,37] In the WICT model, the structural change associated with the ICT process is from planar (sp^2) to pyramidal (sp^3) hybridization of the dimethylamino group N. In the PICT model, a conformation change of amino N from pyramidal (sp^3) to planar (sp^2) is put forward and a planar quinoidal structure is proposed. Rotkiewicz et al.[39] found experimentally that the DMABN derivative *o*-methyl-*p*-cyano-*N*,*N*-dimethylaniline, which has a pretwisted structure in the ground state, showed a twist angle remarkably smaller than 90° in its ICT state. Bernstein et al.[40] also expressed doubts about the fully twisted ICT structure from their supersonic molecular beam studies of DMABN.

(2) The second question concerns the electronic properties of the ICT state: Is the electron donor subgroup, D (supposed to be the dimethylamino group in DMABN), completely decoupled from the acceptor subgroup, A (the benzonitrile group in DMABN), in the ICT state? Zachariasse et al. found that the energy of the F_a emission maximum in a series of dual fluorescent 4-aminobenzonitriles does not show a correlation with the redox potentials of the donor D and the acceptor A. Thus, they concluded that in the ICT state a considerable electronic coupling exists between the A^- and D^+ parts.[24,37]

(3) A further unresolved issue is the conformation of the DE state: Is it planar? A twist angle of 30° for this excited state was deduced from high-resolution laser-induced fluorescence (LIF) excitation spectra measured in a free-jet experiment by Kajimoto et al.[41] The same twist angle was also suggested by Howell et al.[42] and Bernstein et al.[43] in their gas-phase supersonic molecular-beam experiments.

(4) The rate-determining step for the ICT process and the relationship between the rate of formation of the ICT state and solvent dielectric relaxation motion are unclear. One of the criticisms of the TICT model is that the initial evidence for a strong dependence of F_a emission upon viscosity of the solvent[44,45] turned out to be an experimental artifact.[46] From the time dependence of the fluorescence measurements of a series of dialkylaminobenzonitriles, it was found that the ICT rate constant increased with the size of the amino group.[7,11,37] This casts doubt on the TICT argument that the rotation around the $C_{ring}-N(CH_3)_2$ bond is the rate-determining step. Although the importance of the solvent in the anomalous emission mechanism has been specifically considered as due to the sensitivity of the F_a emission maximum and intensity of solvent polarity,[47,48] the effect of solvent in the DMABN ICT process is, in reality, far from completely understood at present.[49]

Numerous theoretical studies using both semi-empirical[9,31,36,50−53] and ab initio[35,54,55] methods have been performed to evaluate the geometric and electronic structures of DMABN in the ground, DE, and ICT states. Besides geometry optimization,[56−58] some elegant theoretical investigations have been made into the evolution of the several lowest-lying potential surfaces (ground-state included) along possible reaction coordinates for the ICT process, both in gas phase[35,54,55] and in solution phase.[9,36,53,59] Most of these studies confirm the validity of the TICT model. However, recently, an alternate relaxation pathway (and thus a different equilibrium structure) of the ICT state was proposed by Sobolewski et al.,[57,60] the so-called RICT model (rehybridization by intramolecular charge transfer). According to this model, the structure of the ICT state consists of an in-plane bent cyano group (rehybridization of the cyano group C atom from sp to sp^2), with the *N*,*N*-dimethylaniline subgroup in almost the same geometry as in the ground state. In a very recent study using refined calculation with more sophisticated basis sets, the RICT model for DMABN could not be validated.[35,54] In the absence of direct experimental data on the structure of excited-state DMABN, these quantum chemical calculations undoubtedly provide very valuable information.

Much of the experimental work, both in solution[5,11,38,61,62] and in jets,[63−65] has focused on the interaction of DMABN with the solvent and the origin of the dual fluorescence. Very little direct information on the structure of DMABN is available from experimental observations to date. Though refined calculations have recently been carried out, these are still limited in providing an accurate, realistic description of the complex ICT processes in DMABN because only a small number of degrees of freedom were considered for geometry optimization, limited reaction coordinates were involved for studying evolution of potential surfaces, and only a very approximate description of solvent

effects was used. Thus, ultrafast structural experimental supporting data are required as has recently been demonstrated.[66]

Time-Resolved Resonance Raman (TR^3) spectroscopy with picosecond time resolution is a powerful method for providing direct geometric and electronic structural information about short-lived species.[67,68] Our long-term program seeks to identify structural changes following an electron-transfer process and determine how such changes stabilize the formation of the ion-pair while restricting the back electron-transfer process. In this paper we report the use of TR^3 spectroscopy to elucidate the structural and electronic properties for the DE and ICT states of DMABN in both nonpolar and polar solvents. Previous attempts have failed because the broad F_a emission present in polar solvents overwhelms the weak Raman signal.[69] To overcome this problem, we have developed an efficient fluorescence rejection technique based on utilization of a Kerr gate.[70] By applying this method we have obtained the first TR^3 spectrum of DMABN in a polar solvent. To select suitable probe wavelengths for the TR^3 experiments, transient absorption (TA) measurements with subpicosecond time resolution for DMABN in various solvents have also been carried out. The Kerr gate has also been used to measure the changes in the wavelength fluorescence profile up to 750 ps with 3 ps time resolution of both the F_a and F_b emissions in polar and nonpolar solvents. The results obtained from our experiments are compared with those from the TICT model and other experimental and theoretical investigations.

2. Experimental Section

The experiments were carried out using TR^3, TA, and time-resolved fluorescence (TRF) setups based on optical parametric amplifiers (OPAs) as described in detail in the literature.[71,72]

The TA measurements were carried out using two independently tunable and synchronized 200−300-fs pulses generated by a regenerative amplifier system operated at 800 Hz. The pump pulses were obtained at 267 nm by frequency-tripling the regenerative amplifier fundamental, providing ~3 μJ after attenuation. A white light continuum generated in a D_2O medium pumped by the regenerative amplifier fundamental was used as a probe. The white light continuum was separated into two beams, one passing through the sample and the other used as a reference. The beams were dispersed on two identical photodiode arrays. The signals from each array were downloaded to a PC and normalized shot-to-shot.

For the TR^3 experiments, samples were pumped by a 277 nm pulse and probed with 415 and 615 nm pulses for the DMABN in polar and nonpolar solvents, respectively. The 277 nm pump and 415 nm probe pulses were the third and second harmonics of the regenerative amplifier fundamental, respectively. The 615 nm probe pulse was generated in the OPA which was pumped by the frequency-doubled output of the regenerative amplifier. The pump and probe pulse durations were ~1 ps, and the pulse energies at the sample were 2−3 μJ. The sample was flowed in a jet with a 500 μm diameter. The pump and probe beams were polarized in parallel and focused to a spot size of approximately 100 μm at the sample. The TR^3 signal was collected at 90° geometry, dispersed through a single spectrograph, and detected by a liquid-nitrogen-cooled charge-coupled device (CCD). A low-fluorescence cutoff and holographic filters were used to block the pump and probe Rayleigh scattered light.

The spectra were fitted using custom-written software.[73] The wavenumber values reported are accurate to ±5 cm^{-1}. The spectra for DE and ICT state DMABN in cyclohexane and methanol (shown in Figures 5 and 6) result from summing 20 individual spectra. Cosmic ray noise was subtracted during data acquisition by using software written specifically for the purpose. Samples were renewed every 2 h during the experiments, and within these time intervals no degradation was observed by UV absorption spectroscopy.

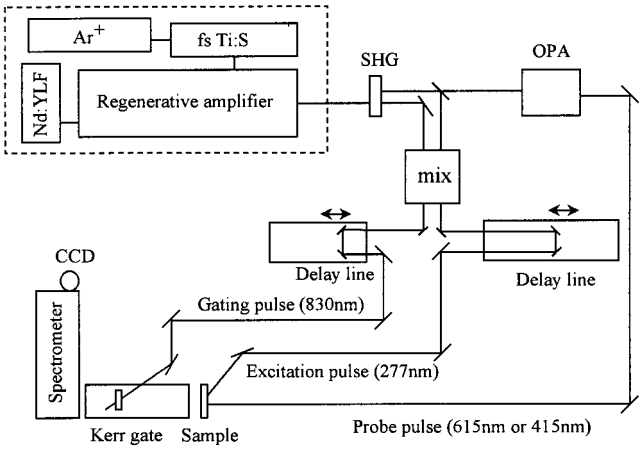

Figure 1. Schematic of our picosecond TR^3 apparatus with the Kerr gate.

Details of the Kerr gated TR^3 setup are given in ref 70. Figure 1 displays the setup diagram of the present TR^3 experiments. Briefly, the separation of Raman signal from fluorescence was achieved in the time domain by using a 3 ps Kerr gate. The Kerr gate consisted of two crossed polarizers and a Kerr medium (CS_2) activated to propagate the Raman signal by using a gating pulse derived from a portion of the regenerative amplifier fundamental (830 nm). The throughput efficiency of the Kerr gate was about 30% (excluding polarizer losses), and the gating duration was about 3 ps when driven by a pulse with 1 ps, 150 μJ pulse energy focused to a spot size of ~1 mm diameter.

For TRF measurements the following changes were made. The Raman probe pulse was blocked and the Kerr gate opened to sample the fluorescence spectrum at various time delays following the excitation pulse. The first collection lens was replaced by a mirror, and benzene was used instead of CS_2 in a 1 mm rather than a 2 mm cell. These modifications reduced dispersion and extended the spectral range into the UV (310 nm). The gate was formed by a UV sheet polarizer (set at the magic angle), the Kerr cell, and a crossed Glan Taylor polarizer. The instrument response time was ~3 ps (rise from 10% to 90%). A 1 cm cell with copper sulfate solution in water was used in front of the spectrometer to block residual scattered light from the gating pulse.

All TR^3, TA, and TRF spectra were obtained by subtracting the negative time-delay background signal from the positive time-delay signal. For TR^3 spectra, the fluorescence background passing through both polarizers when the Kerr gate was open was eliminated from the data by subtracting the signal which had been recorded with no Raman probe pulse present. The TR^3 spectra were calibrated using nonresonant solvent bands and were not corrected for variations in spectral throughput. The TA and TRF spectra were calibrated using 10 nm band-pass filters.

The DMABN and spectroscopic-grade solvents were purchased from commercial sources and used without further purification. The concentrations of the sample solutions were in the range 1−3 mM, and no differences in relative intensity changes within the TR^3 signals were observed up to 10 mM.

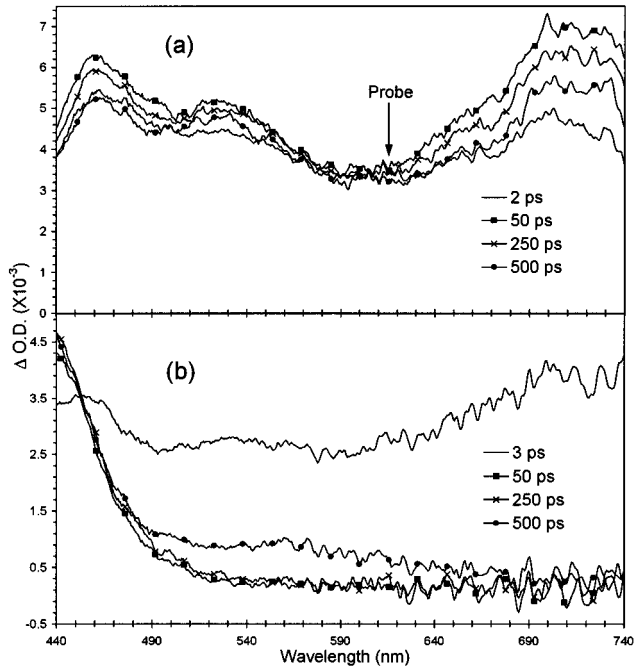

Figure 2. Transient absorption spectra of DMABN in the nonpolar solvent hexane (a) and the polar solvent ethanol (b), obtained at different delay times. The pump laser wavelength was 267 nm.

The nonresonant ground-state Raman spectra of DMABN in hexane and methanol were recorded using an Infinity ISA Raman microspectrometer with 632.8 nm excitation wavelength.

3. Results

3.1. Subpicosecond Transient Absorption Spectroscopy. The TA spectra of DMABN in various solvents were measured in the spectral region 440−740 nm using 267 nm excitation, with the white light continuum probe polarized at the magic angle. The excitation wavelength fell within the strong-absorption band (L_a-type in Platt's notation) of DMABN, which corresponds to the optically allowed S_0 to S_2 ($\pi\pi^*$) transition of the second-lowest energy level. The S_1 state, which is related to the L_b-type band in the F−C region, cannot be directly populated because of its low oscillator strength.[7,55,59,74,75] It should be noted that, along the proposed twist-angle coordinate, S_1 becomes a mainly L_a-type ICT state as the twist angle increases.[9,35,36,53−56] Figure 2 shows typical TA spectra of DMABN in the nonpolar solvent hexane (Figure 2a) and the polar solvent ethanol (Figure 2b) recorded at different time delays.

As shown in Figure 2a, in the nonpolar solvent hexane, the transient spectra display three maxima at 460, 525, and 710 nm, consistent with the observation made by Baumann et al.[32] with slower time-resolution. It is reasonable to attribute the observed absorption to the DE state. The absorption intensity increases until 50 ps following excitation, before decaying (as shown by the 250 and 500 ps spectra) on a time scale consistent with the excited-state lifetime. This increase at early times is not consistent with the TICT model[8] as it stands nor with conclusions drawn from other time-dependent fluorescence studies that propose the DE state as the precursor to the ICT state.[11,38,76−78] As discussed below, we attribute this inconsistency to reverse formation of the ICT state.

For DMABN in the polar solvent, it can be seen from Figure 2b that the TA spectrum is very different from that in the nonpolar solvent. The most significant difference is the change of shape with time. The 3 ps spectrum is similar to the 2 ps spectrum of DMABN in hexane (other polar solvents show the same pattern). This indicates that the same species is present at early time in both solvents, i.e., both the DE and the ICT states as discussed further below. As time evolves, the 3 ps spectrum decays, and an absorption band at about 400 nm (as also present in the TA spectrum of Okada et al.[33]) grows in. Though the maximum of the absorption band is outside our spectral range, the growth of this band can be clearly seen from Figure 2b. The growth lasts for several tens of picoseconds. Detailed kinetic analysis shows that as the 400 nm band decays, a broad absorption around 500−640 nm grows in, indicating a stepwise reaction. This band corresponds to the $T_n \leftarrow T_1$ absorption.[79] For all of the polar solvents investigated (alcohol series, acetonitrile, THF, dioxane, etc.), our TA spectra all display similar behavior, and results are consistent with those obtained by Baumann et al.[32] and Okada et al.[33] We ascribe the late time absorption band at ∼400 nm (>50 ps spectra as shown in Figure 2b) to the ICT state.

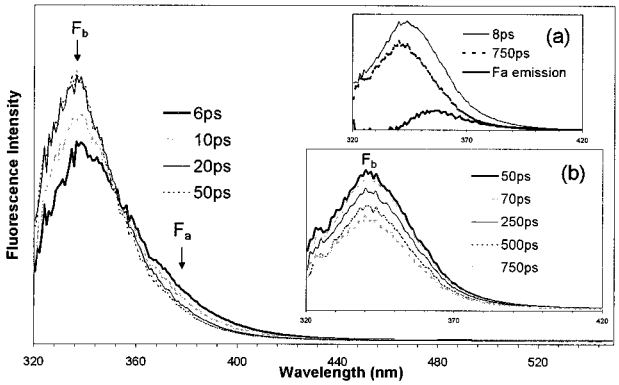

Figure 3. Time-resolved fluorescence spectra of DMABN in hexane recorded at different delay times. The main picture depicts the intensity increase of the F_b fluorescence and the existence of an isosbestic point. Inset (a) displays the early time (8 ps) and late time (750 ps) spectra. The corresponding red fluorescence spectrum is obtained by subtracting the late time spectrum from the early one after normalizing the former with respect to the latter. Inset (b) shows the decay of F_b fluorescence at late decay times.

3.2. Picosecond Time-Resolved Fluorescence Spectroscopy. We have also used the Kerr gate to measure the temporal evolution of the fluorescence profile. The TRF experiments were performed in solvents of different polarities, and the spectra of DMABN in the nonpolar solvent hexane and the polar solvent ethanol are displayed in Figures 3 and 4, respectively. It is clear that in both solvents the shapes of the spectra are similar at early time, consistent with our TA measurements in the corresponding solvents. This suggests that both the F_a and F_b fluorescence emission bands are present at early times in both polar and nonpolar solvents. As shown in Figure 3, the F_b fluorescence dominates at late delay times, whereas the spectra in Figure 4 show that the F_a fluorescence dominates at long delay times. The appearance of isosbestic points in both spectra suggests two interconverting distinct species are present, namely the DE and the ICT states of DMABN.[11,38]

3.3. Picosecond Time-Resolved Resonance Raman Spectroscopy. From our TA measurements, the probe wavelength of 615 nm was chosen for the TR^3 experiments on the DE state of DMABN (nonpolar solvent) and 415 nm for the ICT state (polar solvent). A 50 ps delay time was selected for recording TR^3 spectra of both the DE and ICT states.

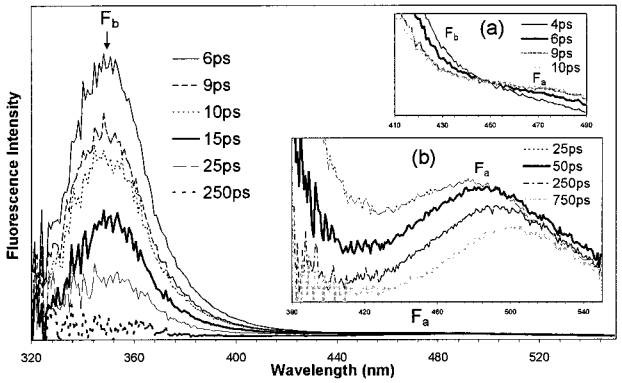

Figure 4. Time-resolved fluorescence spectra of DMABN in ethanol recorded at different delay times. The main picture shows the early time spectra and the rapid decay of F_b fluorescence. Inset (a) shows an isosbestic point during the ICT process at early times. Inset (b) depicts the dynamic Stokes shift of the F_a fluorescence at late delay times.

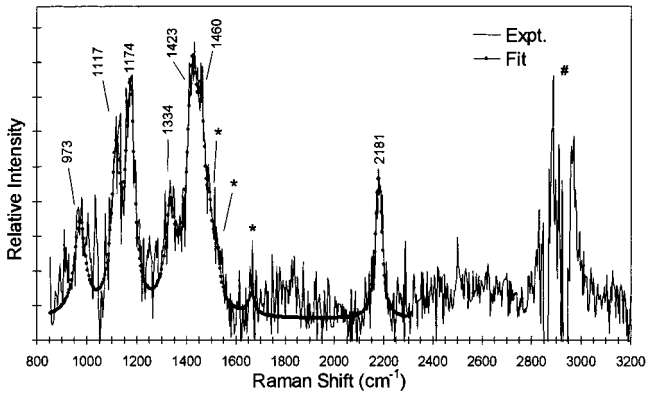

Figure 5. Time-resolved resonance Raman spectrum of the DE-state DMABN obtained for DMABN in cyclohexane solvent, with a 277 nm pump, 615 nm probe, at 50 ps time delay. The bands marked by "*" are not fully established. Solvent subtraction artifact is labeled by "#".

The TR^3 spectra of DE-state and ICT-state DMABN in the spectral region 800−3200 cm^{-1} are shown in Figures 5 and 6, respectively. Both spectra have solvent and fluorescence backgrounds subtracted. Due to the relatively weak transient absorption and the strong fluorescence, the DE-state spectrum shown in Figure 5 took 10 h to accumulate while the ICT-state spectrum shown in Figure 6 took 45 h.

The transient Raman bands were fitted to Lorentzian line shape.[73] For the TR^3 spectra of the DE and ICT states, the fitted band frequencies, relative intensities, and tentative assignments are given in Tables 1 and 2, respectively. Modes related to phenyl ring vibrations are referred to using Wilson notation. Our assignment is based on the normal coordinate analysis of DMABN performed by Gates et al.[80] and Schneider et al.[81] and our comparison with the previously reported spectra of related compounds.[82−87] For comparison, corresponding information on the Raman spectra of ground-state DMABN (in nonpolar solvent), the DMABN radical cation,[88] aniline radical cation,[82c,89] and 3,5 DMDMA radical cation[87] is included in Table 1, and that of ground-state DMABN in polar solvent in Table 2.

3.3.1. DE State. The TR^3 spectrum of DE-state DMABN presented in Figure 5 was obtained in cyclohexane solvent with a 277 nm pump, 615 nm probe at 50 ps pump, and probe pulse time delay. As interpreted above, under such experimental conditions, the observed transient Raman bands originate from the population of the DE state of DMABN. To confirm that the observed bands are not due to poor solvent-band subtraction, the same experiment was repeated in fully deuterated cyclohexane, which has no strong Raman solvent band in the ranges 1300−1900 and 2500−3200 cm^{-1}, and no spectral differences were observed. Furthermore, the same spectrum was also recorded in hexane.

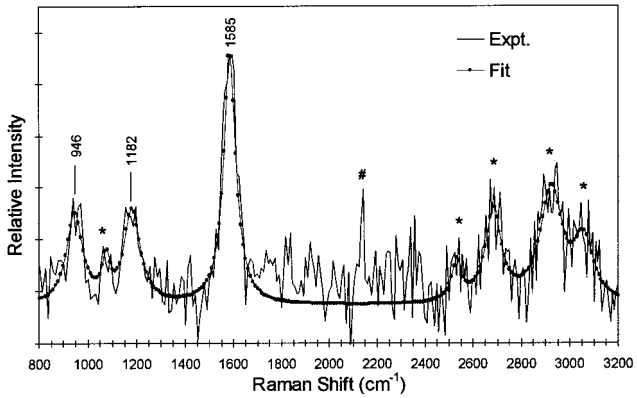

Figure 6. Time-resolved resonance Raman spectrum of the ICT-state DMABN obtained for DMABN in methanol solvent, with a 277 nm pump, 415 nm probe, at 50 ps time delay. The bands indicated by "*" are not fully established. Cosmic ray artifact is labeled by "#".

In general, the main spectral feature shown in Figure 5 is similar to that of the resonance Raman spectrum of the aniline radical cation[82c] and the phenoxyl radical.[82b,d] The 1423 cm^{-1} band is the strongest in the spectrum and was assigned to predominantly $C_{ring}-N(CH_3)_2$ stretching vibrational mode (Wilson 7a), although some contributions from the ring C−H bending (Wilson 19a) and methyl deformation motions are possibly involved.[80, 86] The same mode with the same frequency has also been observed for the *p*-phenylenediamine radical cation,[90] from which the bond order of $C_{ring}-N$ bond was evaluated to be 1.5. The 1423 cm^{-1} frequency is higher than that of the counterpart bands for both ground-state DMABN (Table 2) and DMABN radical cation (Table 1), which are 1373 and 1402 cm^{-1}, respectively. A recent X-ray diffraction analysis[91] established that the structure of the DMABN crystal is not planar, but is pyramidal in the ground state. The dimethylamino group N atom was found to have pyramidal character, with a value of 11.9° (wagging angle) for the angle between the plane of the amino group and the phenyl ring. By contrast, the resonance Raman investigation of DMABN radical cation[88] suggested a semiquinoidal planar structure based on the frequency increase of 7a mode in comparison with that in the ground state, and a partial double bond character of the $C_{ring}-N$ bond. Thus, the double bond character is more obvious in the DE state of DMABN than in the DMABN radical cation. This indicates a considerable tightening of the $C_{ring}-N(CH_3)_2$ bond in the DE state. A similar observation was found by Kajimoto et al. in the gas phase.[41] From Table 1, it can be seen that 3,5 DMDMA radical cation shows the similar 7a mode frequency (1420 cm^{-1}) indicating a similar $C_{ring}-N$ bond strength. The frequency of this mode in the aniline radical cation is 1494 cm^{-1} (Table 1) with the $C_{ring}-N$ bond order greater than 1.5.[82c,89] The lowering of the 7a frequency for the DE state of DMABN relative to that in the aniline radical cation might be due to the interaction between the lone pair orbital of the amino N atom with the orbitals of methyl groups, as discussed by Brouwer and Wilbrandt.[86]

The structure of the aniline radical cation is revealed to be a planar conformation[82c] which is similar to the structure of phenoxyl radical.[82b] Also the planar structure was concluded

TABLE 1: Vibrational Frequencies and Tentative Assignments of the DMABN DE-State Time-Resolved Resonance Raman Spectrum (DMABN in Cyclohexane, 277 nm Pump, 615 nm Probe, 50 ps Time Delay)

tentative assignment		vibrational frequency				
approximate description	Wilson mode	DMABN DE state in cyclohexane,[a] this work	3,5 DMDMA radical cation[e]	$C_6H_5NH_2$ radical cation[a,b]	DMABN radical cation in EtOH, 77 K[a,c]	DMABN ground state in hexane,[a,d] this work
ring breadth	1	*f*			808 (m)	785 (m)
N−$(CH_3)_2$ stretch(s)		973 (41)	975		964 (m)	
CH_3 rocking		1117 (53)	1159			
ring C−H in-plane bend	9a	1174 (70)		1175 (8)	1186 (m)	1179 (m)
C═C stretch	3	1334 (37)		1338		
CH_3 deformation			1370			
C_{ring}−N stretch	7a	1423 (100)	1420	1494 (100)	1402 (m)	
δ CH_3		1460 (36)	1435			
C═C stretch	19a		1482	1528 (8)	1522 (s)	
C═C stretch	8a		1571	1574 (15)	1624 (m)	1608 (s)
C≡N stretch		2181 (37)			2214 (m)	2220 (vs)

[a] Relative intensities are given in parentheses along with frequencies. [b] References 82c and 89. [c] Reference 88. [d] Values from normal Raman spectrum of ground-state DMABN in hexane solution excited at 632.8 nm. [e] Reference 87. [f] Because of the effect of the filter, Raman bands below 800 cm^{-1} cannot be detected.

TABLE 2: Vibrational Frequencies and Tentative Assignments of the DMABN ICT State Time-Resolved Resonance Raman Spectrum (DMABN in Methanol, 277 nm Pump, 415 nm Probe, 50 ps Time Delay)

tentative assignment		vibrational frequency (cm^{-1})		
			ground state	
approximate description	Wilson mode	ICT state DMABN in MeOH[a], this work	DMABN in MeOH[a,b], this work	DMABN in EtOH excited at 488 nm[c]
ring breadth	1	*d*	784 (m)	788
ring out-of-plane C−H bending	5	946 (47)		946[e]
ring in-plane C−H bend	9a	1182 (48)	1180 (m)	1184
C_{ring}−N stretch	7a			1373
C═C stretch	19a			1532
C═C stretch	8a	1585 (100)	1607 (s)	1608
C≡N stretch			2214 (vs)	2215[e]

[a] Relative intensities are given in parentheses along with frequencies. [b] Values from normal Raman spectrum of ground-state DMABN in methanol solution excited at 632.8 nm. [c] Reference 88. [d] Because of the effect of the filter, Raman bands below 800 cm^{-1} cannot be detected. [e] Observed from IR spectrum. See ref 81.

for 3,5 DMDMA radical cation[87] and DMA radical cation from both the experiments and calculation.[86,87] Therefore, we suggest a planar conformation for the DE-state DMABN. Given the pyramidal structure in the ground state,[91] this indicates a geometry change from a nonplanar to a planar structure for DMABN on going from the ground state to the DE state.

The 1174 and 1334 cm^{-1} bands (Figure 5) were assigned to the pure phenyl ring C−H bending vibration (Wilson 9a) and non-totally symmetric C═C stretching mode (Wilson 3), respectively. The latter assignment is based upon Brouwer and Wilbrandt's analysis of the resonance Raman spectra of dimethylaniline radical cation and aniline radical cation.[86] An alternative assignment for the 1334 cm^{-1} band is the methyl group deformation vibration mode, as the tentative assignment suggested by Poizat et al.[87] (Table 1).

From Table 1, the comparison with DMABN radical cation and 3,5 DMDMA radical cation seems to suggest the assignment of the 973 cm^{-1} band to the N−$(CH_3)_2$ stretching mode of the DE state of DMABN (Figure 5). However, in light of more recent normal-mode analysis of the ground-state DMABN presented by Schneider et al.,[81] assignment of the corresponding ground-state band at 946 cm^{-1} (Table 2) to N−$(CH_3)_2$ stretching vibration made by Gates et al.[80] is no longer believed to be valid, and we reassigned the band to the phenyl ring mode Wilson 5. According to the harmonic-vibrational frequency calculation of the similar species, *N*,*N*-dimethylaniline radical cation and its various isotopic derivatives,[86] the band appearing at this frequency range corresponds to the phenyl ring mode Wilson 12, although no experimental observations were made. But, the gas-phase LIF experiments on DMABN assigned a low-frequency band at about 500 cm^{-1} to Wilson 12[56] for the DE state of DMABN. To resolve this ambiguity, deuterated DMABN experiments will be carried out.

As shown in Figure 5, a high intensity shoulder near the 7a band is present at 1460 cm^{-1}. This frequency coincides with the methyl group deformation vibration δCH_3 (in Table 1), and this is insensitive to the parent group.[85,92] Referring to the normal-mode analysis,[80,81] the 1117 cm^{-1} band is tentatively assigned to the dimethylamino group methyl in-plane rocking motion. As discussed by Poizat et al.,[87] the activity of the vibrations of alkyl group for the radical cation of dimethylaniline and its derivatives can be taken as characteristic of ($^+$N═) for the nitrogen bonding configuration in aromatic amines. This is assumed to result from the couplings between the alkyl group and the π chromophore.

The middle intensity band at 2180 cm^{-1} clearly belongs to the C≡N stretching mode. The ~40 cm^{-1} frequency downshift on going from the ground state to the DE state (Table 1)

indicates a partial charge-transfer character for this state.[67,93] This is consistent with the TICT model[17,18] and theoretical analyses.[9,55,59]

3.3.2. ICT State. The TR^3 spectrum of the ICT-state DMABN, shown in Figure 6, was obtained in methanol with a 277 nm pump, 415 nm probe at 50 ps pump, and probe pulse time delay. As described above, the observed transient Raman bands originate from the population of the ICT state. Although the 415 nm probe wavelength is not within the monitored spectral range (Figure 2b), it is near to the maximum of the first $S_n \leftarrow S_1$ TA band (the second band is around 320 nm) for DMABN in polar solvents. This can be seen from the transient absorption spectrum recorded by Okada et al.[33] in the spectral range from 300 to 480 nm. Transient resonance Raman bands under these conditions thus obtain their resonance enhancement from the corresponding electronic transition. Because of the large red shift of the F_a fluorescence for DMABN in methanol, this means the TR^3 spectrum with the best S/N ratio was obtained in this solvent. Similar spectra, not illustrated, were also recorded in ethanol and acetonitrile solvents. Considering the different polarities of the alcohol solvents and the aprotic nitrile solvent ($\epsilon = 32.66$ for methanol, $\epsilon = 24.55$ for ethanol, and $\epsilon = 35.94$ for acetonitrile),[94] we suggest that the conformation of the ICT-state DMABN in polar solvents, at least in comparably strong polar solvent, is essentially the same. Okada et al.[33] presented the same argument based on the calculated transition moments, μ_f, of the F_a emission which were found to be independent of solvent polarity. We also obtained the same TR^3 spectrum for the ICT state in deuterated alcohol. This isotope substitution experiment indicates that the isotopic effects previously observed in fluorescence experiments are attributed mainly to the dynamics of the ICT reaction, especially radiationless intramolecular processes, such as intersystem crossing and internal conversion,[79,95] and do not influence the structure of the ICT state. It should be pointed out that the ICT state detected in the present TR^3 experiment is the final solvent-equilibrated state. It is known that besides internal coordinates, such as rotation of amino group, solvent reorganization is an important reaction coordinate.[25] Though Su and Simon[49] pointed out the importance of fluctuations of intramolecular vibrational motion compared to solvent diffusion in determining the reaction rates in a series of alcohol solvents, a specific solute−solvent interaction has been postulated by several authors.[6,22,96] Our recent TRF measurements, to be fully reported elsewhere, showed that the dynamic shift of the F_a fluorescence continued for several hundreds of picoseconds in long-chain alcohol solvents, which is attributable mainly to the solvent reorientation relaxation.[97] However, because of the large dielectric constant and the short solvation time (5 ps)[100] of methanol, both the ICT reaction and the solvation process are expected to have already finished at the 50 ps delay time.[97]

As displayed in Figure 6, the spectral features of the ICT state are distinctly different from those of the DE state (Figure 5). In the 800−2400 cm^{-1} frequency range, the ICT-state spectrum is composed of a strong band at 1583 cm^{-1} and two relatively weak bands at 1182 and 946 cm^{-1}. However, at the 2000−2200 cm^{-1} range, corresponding to the frequency of the C≡N stretching mode,[66,93] no reproducible feature was recorded.

It can be seen from Figure 6 that the 1585 cm^{-1} band is the most intense. According to a previous calculation,[54] the C≡N stretching mode of the ICT state in the RICT model is predicted to be downshifted to 1649 cm^{-1}, which is near the 1585 cm^{-1} band. However, the frequency of the C≡N stretching vibration was found at 2096 cm^{-1} by Hamaguchi,[93] and recently by picosecond time-resolved infrared experiment.[66] We therefore assign the 1585 cm^{-1} band to the phenyl ring C═C stretching mode Wilson 8a (Table 2). The 23 cm^{-1} frequency downshift on going from the ground state to the ICT state indicates the weakening of the C═C bond in the latter case. This is in agreement with the results of several refined ab initio calculations,[35,54,56] which showed increased size of the phenyl ring and lengthened distance between C_1-C_4 in the ICT state. The other ring mode, 1182 cm^{-1}, is assigned to the pure C−H bending mode Wilson 9a, this mode being insensitive to substitution. This band is the only one with almost the same frequency in all the states, i.e., ground, DE, and ICT state. The ground-state 946 cm^{-1} band appears at the same frequency as in the ICT state. The assignment of this band warrants further investigation in light of the work by Schneider et al.[81] Furthermore, the intensity of this band in the presented spectrum may have been diminished because of the spectral cutoff filter, and thus its relative intensity is probably higher than that recorded. At this stage, because of the poor signal-to-noise ratio we do not attempt to assign any of the other weaker features observed within the spectra. These bands are marked with asterisks within Figure 6.

When comparing the TR^3 spectra of the DE state (Figure 5) and the ICT state (Figure 6) of DMABN, the most notable difference is the absence of the broad 1423 cm^{-1} band, which is the strongest one in the DE state, and the absence of the C≡N mode in the ICT spectrum. This may indicate localization of the chromophore in resonance with probe wavelength on the phenyl ring.

4. Discussion

4.1. Transient Absorption and Fluorescence Spectroscopy. Transient absorption represents an optical transition from a lower excited state to the F−C states of upper potential surfaces. The absorption intensity change with time reflects the change of population of the absorbing excited state. In the case of DMABN in a nonpolar solvent, this state corresponds to the DE state, which is an L_b-type state on the S_1 surface.[25,32] As mentioned above, the initially excited state is the L_a-type S_2 state and to reach the L_b-type S_1 surface an internal conversion is needed; this is supported by both experimental[15,98] and theoretical work.[9,55] Our TRF measurements show, in Figure 3, that both F_a and F_b fluorescence bands are present at early times (<50 ps), and we suggest that this is because the ICT and DE states are rapidly populated by the internal conversion process. Mechanistically, the intensity increase of the F_b fluorescence as the F_a fluorescence intensity decreases, and the presence of an isosbestic point (Figure 3), are evidence that the ICT state decays rapidly to the DE state; i.e., the reverse charge-transfer process from the ICT state to DE state is occurring.[97] The importance of the reverse ICT reaction has been pointed out by Zachariasse et al.[11,38] Using the continuum models of Onsager to describe the solute−solvent interaction, the theoretical study performed by Gorse et al.[9] showed that the barrier for the ICT reaction (ΔE of DE→ICT) is independent of solvent polarity, whereas the reverse barrier (ΔE of ICT→DE) is strongly solvent polarity dependent, being small in nonpolar solvent. This is consistent with our TRF results. Therefore, we deduce that the observed intensity increase of TA bands at early delay times is caused by the reverse ICT→DE process. Although we cannot completely rule out the possibility that the early red-shifted fluorescence is due to IVR, this interpretation seems unlikely as our TRF spectra exhibit a clear isobestic point, implying the presence of two distinct interchanging states. This is the first

direct experimental evidence for the population increasing of the DE state at short times following electronic excitation. In previous time-dependence fluorescence measurements performed on DMABN[5,6,7,98] it was always found that the F_b fluorescence decayed immediately upon the excitation. We believe this is because (i) the behavior of DMABN in nonpolar solvent has been much overlooked in previous work investigating the origin of the F_a emission, (ii) the slower time resolution in previous studies obscured the real rise time of the F_b fluorescence, and (iii) the overlap of the F_a and F_b fluorescence below 400 nm prevents accurate measurement of the fluorescence decay profile by the time-dependence fluorescence experiments performed at a fixed wavelength.

Previous time-resolved studies of the dual fluorescence of DMABN indicate that the equilibrium between the DE and ICT states occurs within the excited-state lifetime,[6,11,38,98] and our results are in agreement with this. For DMABN in nonpolar solvent, the charge transfer takes place but the ICT state is not stabilized, so that the F_b fluorescence dominates at later times. In contrast, for polar solvents the initially formed DE state rapidly changes to the ICT state, and this is stabilized by the dielectric interaction of the polar solvents. Taking into consideration that no F_a fluorescence has been observed for isolated DMABN or even for 1:1 complexes of DMABN with nonpolar or polar solvent molecules in the gas phase,[40,41,43,64,65] the existence of both F_a and F_b fluorescence in both polar and nonpolar solvents indicates that the dielectric interaction between excited-state DMABN and solvent molecules in a solution environment is important for the ICT process, and the longitudinal relaxation of the solvent influences the ICT reaction. The former allows the charge-transfer process to occur in the nonpolar solvent and is thus in accordance with an inner-sphere process of the Sumi−Nadler−Marcus definition,[99] while in the polar solvent ethanol the initially formed charge-transfer state is further stabilized by the reorientational relaxation of the surrounding solvent. This includes the outer-sphere solvent relaxation as indicated by the large dynamic Stokes shift of the F_a fluorescence (Figure 4b). However, in ethanol, kinetic analysis suggests that the reaction rate is not limited by the solvation time. That is, the time for the ICT reaction is ∼8 ps while the average solvation time for ethanol is ∼16 ps.[100] This indicates that the impetus for the charge separation comes from the DMABN intramolecular relaxation as well as the solvent dielectric response, in agreement with the results of Su and Simon.[49] The fluorescence studies will be fully reported elsewhere; for this work we limit our interpretation to the above.

4.2 Time-Resolved Resonance Raman Spectroscopy. 4.2.1. DE State. *4.2.1.1. Geometric Structure.* Though there are similarities between our results and those of free-jet molecular-beam experiments,[41,43] such as the contraction of the $C_{ring}-N(CH_3)_2$ bond, the planar structure we put forward is in contradiction with the structure deduced from gas-phase studies. A structure with a 30° twisted angle (the torsional angle between the plane of the dimethylamino group and that of the phenyl ring) and a 0° wagging angle has been suggested by several authors.[41−43] However, as discussed by Kajimoto et al.,[41] the estimation of this angle was subject to significant uncertainty because the simulated spectra were rather insensitive to the angle. This was well explained by a theoretical study performed by Roos et al.[55] and Gorse et al.[9] They found that in the gas phase the potential curve for the DE state is very flat for a motion of 0−30° along the twist angle coordinate.[55] This implies a very small torsional barrier up to 30° in the gas phase. However, by including solvent effects, Gorse et al.[9] showed that the shape of the DE state potential curve becomes steep as the twist angle in both polar and nonpolar solvent is increased, with a steeper slope in polar solvents. Undoubtedly, this causes the planar structure (with 0° twisting angle) to be the most stable conformation for the DE state in solution. This interpretation is in good agreement with our result. The planar structure of the DE state was verified again by the recent calculation.[66]

4.2.1.2. Electronic Property. One of the main goals of our investigation is to understand the electronic properties of the DE and ICT states, which is very important for elucidating the charge-transfer process in the excited state of DMABN. As mentioned above, the frequency increase of the Wilson 7a vibration implies the shortening of the $C_{ring}-N(CH_3)_2$ bond length, and clearly indicates the overlap of the amino N atom lone pair orbital with the π system of the phenyl ring. This means an increased delocalization of the electron distribution in comparison to the ground state, and a conjugated character in this DE state, as was also concluded by Kajimoto et al.[41] and the theoretical studies using both semiempirical[9,50] and ab initio[35,55] methods. Furthermore, this reasoning favors describing the excited state as a delocalized excited (DE) state rather than a local excited (LE) state.

One interesting question is whether the cyano group is a part of the conjugated system. The answer is affirmative in the TICT model[17,18] and some theoretical work.[9,50] However, our TR^3 evidence appears to be inconsistent with these conclusions. We suggest this because of the lack of the characteristically high-intensity Wilson 8a mode, which always shows as the strongest band in the resonance Raman spectra of compounds possessing quinoidal[101,102] or semiquinioidal[103,104] structures and indicates that the cyano group is not significantly involved in the conjugated system. For example, in *p*-$(CH_3)_2NC_6H_4N(CH_3)_2$,[105] and the *p*-$NH_2C_6H_4OCH_3$ radical,[82e] etc., the full conjugated system includes both of the para-substituents. The similarity between the spectral feature of the DE-state DMABN and that of the aniline radical cation[82c] and the phenoxyl radical[82b] also implies that the cyano group does not perturb the electronic transition very much. One explanation for the absence of the Wilson 8a mode may be that this vibration is not resonantly enhanced at the 615 nm probe wavelength. However, from the above description (section3.3.1), it is clear that all of the dimethylamino group, phenyl ring, and cyano group are part of the chromophore. It is thus reasonable to expect that the phenyl ring C═C stretching vibration (the characteristic quinoidal mode 8a) should be resonance-enhanced if the DE state of DMABN is similar in nature to fully conjugated systems with para-substituents. In fact, in molecular orbital calculations,[66] the bond length of $C_{ring}-C_{cyano}$ was found to be longer in the DE state than in the ground state, but the $C_{ring}-N(CH_3)_2$ bond length was found to become notably shorter on going from the ground state to the DE state.[9,56,66] This was believed to indicate that conjugation between the N atom lone pair orbital and the phenyl ring π system is important.[9,55,56,66]

On the basis of the above discussion, we conclude that in the DE state, the cyano group does not participate in the conjugated system composed of the dimethylamino group and the phenyl ring. Forster et al.[88] drew the same conclusion for the DMABN radical cation. They attribute this to the electron-withdrawing property of the cyano group. It was pointed out that the ability only to withdraw but not to donate electrons to an attached conjugated molecular system is fully conserved for the cyano group in the DMABN radical cation system. Our spectral observations here imply that the case in the DE state of DMABN is similar.

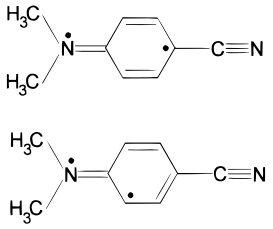

Figure 7. Suggested structures for the DE-state DMABN.

Taking into consideration both the geometric and electronic properties, the structure of the DE state suggested here is best represented by canonically planar structures[83] with the cyano group isolated from the conjugated system and double bond character for the $C_{ring}-N(CH_3)_2$ bond (see Figure 7).

4.2.2. ICT State. As mentioned in the Introduction, four main models have been put forward in an attempt to interpret the wealth of experimental observations: TICT, WICT, PICT, and RICT. The RICT model has been ruled out by previous time-resolved infrared experiments[66,93] and high-level theoretical calculations.[35,54] The discrimination among the remaining three models is an ongoing controversy. The resonance Raman spectrum presented here (Figure 6) does not provide enough evidence to reach the long-sought-after conclusion. We believe the absence of a C≡N stretching band in our TR^3 spectrum of the DMABN ICT state indicates a substantial change within the electronic nature of the ICT state in comparison to the DE state and is possibly accompanied by a structural change in relation to the planar DE state. This casts some doubt on the PICT model, which proposes the pyramidal structure of the DE state, and emphasizes that the planarization of the dimethylamino group, i.e., changing from pyramidal to planar structure, is the critical intramolecular coordinate for changing from the DE state to the ICT state.[24,37] Many theoretical works[9,35,36,55,59] give prominence to the TICT model as the sole intramolecular reaction coordinate for converting from the DE to the ICT state, in particular excluding the WICT model. However, as suggested by Parusel et al.,[35] the combination of the TICT and WICT is still possible for the ICT reaction. Moreover, much evidence has been found in favor of a partially twisted ICT state rather than a 90° perpendicular conformation.[33,35,38,54,59] To elucidate these questions, further time-resolved vibrational spectra studies are required.

5. Conclusion

In the present work we have studied the electronic and structural nature of the DE and ICT states of DMABN with a range of picosecond time-resolved techniques. By using a Kerr gate to reject fluorescence, the TR^3 spectrum of DMABN in polar solvent has been obtained for the first time. The TA and the TRF spectra of DMABN in various solvents have also been recorded with subpicosecond and picosecond time resolution, respectively. The TR^3 spectrum of the DE state is consistent with a planar structure with obvious double bond character in the $C_{ring}-N(CH_3)_2$ bond (bond order 1.5). A canonical electronic structure with the cyano group isolated from the conjugated system (comprising the dimethylamino group and the phenyl ring) is suggested for the DE state. The TR^3 spectrum of the ICT state DMABN is dominated by a band assigned to the phenyl ring C═C stretching vibration. The frequency downshift of this mode relative to the ground state indicates loosening of the phenyl ring. Our TA spectra are in agreement with those obtained by Okada et al.[33] The unexpected increase in the TA intensity at early delay times for DMABN in nonpolar solvent is attributed to a reverse population of the DE state from the ICT state. Our TRF spectra support these conclusions.

Acknowledgment. We are grateful to the EPSRC for financial support. W.M.K gratefully acknowledges financial support from the Croucher foundation, Hong Kong. This work was carried out within the Central Laser Facility, CLRC Rutherford Appleton Laboratory.

References and Notes

(1) Lippert, E.; Luder, W.; Boos, H. In *Advances in Molecular Spectroscopy; European Conference on Molecular Spectroscopy, Bologna 1959;* Mangini, A., Ed.; Pergamon Press: Oxford, 1962; p 443.
(2) Lippert, E.; Rettig, W. *J. Mol. Struct.* **1978**, *45*, 373.
(3) Grabowski, Z. R.; Rotkiewicz, K.; Rubaszewska, W.; Kaminska, E. K. *Acta Phys. Pol., A* **1978**, *54*, 767.
(4) Khalil, O. S.; Hofeldt, R. H.; McGlynn, S. P. *J. Lumin.* **1973**, *6*, 229.
(5) Weisenborn, P. C. M.; Huizer, A. H.; Varma, C. A. G. O. *Chem. Phys.* **1988**, *126*, 425.
(6) Wang, Y.; Eisenthal, K. B. *J. Chem. Phys.* **1982**, *77*, 6076.
(7) Zachariasse, K. A.; Grobys, M.; Von der Haar, T.; Hebecker, A.; Ilchev, Y. V.; Jiang, Y.-B.; Morawski, O.; Kuhnle, W. *J. Photochem. Photobiol., A: Chem.* **1996**, *102*, 59.
(8) Rettig, W. *Proc. Indian Acad. Sci., Chem. Sci.* **1992**, *104*, 89.
(9) Gorse, A.-D.; Pesquer, M. *J. Phys. Chem.* **1995**, *99*, 4039.
(10) Platt, J. R. *J. Chem. Phys.* **1949**, *17*, 484.
(11) Schuddeboom, W.; Jonker, S. A.; Warman, J. M.; Leinhos, U.; Kuhnle, W.; Zachariasse, K. A. *J. Phys. Chem.* **1992**, *96*, 10809.
(12) Weisenborn, P. C. M.; Varma, C. A. G. O.; De Haas, M. P.; Warman, J. M. *Chem. Phys. Lett.* **1986**, *129*, 562.
(13) Grabowski, Z. R. *Pure Appl. Chem.* **1993**, *65*, 1751.
(14) Wiessner, A.; Huttmann, G.; Kuhnle, W.; Staerk, H. *J. Phys. Chem.* **1995**, *99*, 14923.
(15) Rettig, W.; Wermuth, G. *J. Photochem.* **1985**, *28*, 351.
(16) Lippert, E.; Luder, W.; Moll, F.; Nagele, H.; Boos, H.; Prigge, H.; Siebold-Blankenstein, I. *Angew. Chem.* **1961**, *73*, 695.
(17) Rotkiewicz, K.; Grellmann, K. H.; Grabowski, Z. R. *Chem. Phys. Lett.* **1973**, *19*, 315.
(18) Grabowski, Z. R.; Rotkiewicz, K.; Siemiarczuk, A.; Cowley, D. J.; Baumann, W. *Nouv. J. Chim.* **1979**, *3*, 443.
(19) Kosower, E. M.; Dodiuk, H. *J. Am. Chem. Soc.* **1976**, *98*, 924.
(20) Nakashima, N.; Mataga, N. *Bull. Chem. Soc. Jpn.* **1973**, *46*, 3016.
(21) Visser, R. J.; Varma, C. A. G. O.; Konijnenberg, J.; Bergwerf, P. *J. Chem. Soc., Faraday Trans. 2* **1983**, *79*, 347.
(22) Visser, R. J.; Varma C. A. G. O. *J. Chem. Soc., Faraday Trans. 2* **1980**, *76*, 453.
(23) Zachariasse, K. A.; Von der Haar, T.; Leinhos, U.; Kuhnle, W. *J. Inf. Rec. Mater.* **1994**, *21*, 501.
(24) Zachariasse, K. A.; Grobys, M.; Von der Haar, T.; Hebecker, A.; Ilchev, Y. V.; Morawski, O.; Ruckert, I.; Kuhnle, W. *J. Photochem. Photobiol., A: Chem.* **1997**, *105*, 373.
(25) Lippert, E.; Rettig, W.; Bonacic-Koutecky, V.; Heisel, F.; Miehe J. A. *Adv. Chem. Phys.* **1987**, *68*, 1.
(26) Kohler, G.; Rotkiewicz, K. *Spectrochim. Acta* **1986**, *42A*, 1127.
(27) (a) Rettig, W.; Wermuth, G.; Lippert, E. *Ber. Bunsen-Ges. Phys. Chem.* **1979**, *83*, 692. (b) Rettig, W.; Lippert, E. *J. Mol. Struct.* **1980**, *61*, 17.
(28) Sinha, H. K.; Muralidharan, S.; Yates, K. *Can. J. Chem.* **1992**, *70*, 1932.
(29) Rotkiewicz, K.; Rubaszewska, W. *Chem. Phys. Lett.* **1980**, *70*, 445.
(30) Rettig, W.; Braun, D.; Suppan, P.; Vauthey, E.; Rotkiewicz, K.; Luboradzki, R.; Suwinska, K. *J. Phys. Chem.* **1993**, *97*, 13500.
(31) Khalil, O. S.; Meeks, J. L.; McGlynn, S. P. *Chem. Phys. Lett.* **1976**, *39*, 457.
(32) Okada, T.; Mataga, N.; Baumann, W. *J. Phys. Chem.* **1987**, *91*, 760.
(33) Okada, T.; Uesugi, M.; Kohler, G.; Rechthaler, K.; Rotkiewicz, K.; Rettig, W.; Grabner, G. *Chem. Phys.* **1999**, *241*, 327.
(34) Rulliere, C.; Grabowski, Z. R.; Dobkowski, J. *Chem. Phys. Lett.* **1987**, *137*, 408.
(35) Parusel, A. B. J.; Kohler, G.; Grimme, S. *J. Phys. Chem.* **1998**, *102*, 6297.
(36) Broo, A.; Zerner, M. C. *Chem. Phys. Lett.* **1994**, *227*, 551.
(37) Von der Haar, T.; Hebecker, A.; Ilichev, Y.; Jiang, Y.-B.; Kuhnle, W.; Zachariasse, K. A. *Recl. Trav. Chim. Pays-Bas* **1995**, *114*, 430.
(38) Leinhos, U.; Kuhnle, W.; Zachariasse, K. A. *J. Phys. Chem.* **1991**, *95*, 2013.
(39) Rotkiewicz, K. *Spectrochim. Acta* **1986**, *42A*, 575.

(40) Warren, J. A.; Bernstein, E. R.; Seeman, J. I. *J. Chem. Phys.* **1988**, *88*, 871.
(41) Kajimoto, O.; Yokoyama, H.; Ooshima, Y.; Endo, Y. *Chem. Phys. Lett.* **1991**, *179*, 455.
(42) Howells, B. D.; McCombie, J.; Palmer, T. F.; Simons, J. P.; Walters, A. *J. Chem. Soc., Faraday Trans. 2* **1992**, *88*, 2603.
(43) Grassian, V. H.; Warren, J. A.; Bernstein, E. R.; Secor, H. V. *J. Chem. Phys.* **1989**, *90*, 3994.
(44) Struve, W. S.; Rentzepis, P. M. *J. Chem. Phys.* **1974**, *60*, 1533.
(45) Struve, W. S.; Rentzepis, P. M. *J. Chem. Phys.* **1973**, *59*, 5014.
(46) (a) Hicks, J. M.; Vandersall, M. T.; Sitzmann, E. V.; Eisenthal, K. B. *Chem. Phys. Lett.* **1987**, *135*, 413. (b) Hicks, J. M.; Vandersall, M. T.; Babarogic, Z.; Eisenthal, K. B. *Chem. Phys. Lett.* **1985**, *116*, 18.
(47) Struve, W. S.; Rentzepis, P. M. *Chem. Phys. Lett.* **1974**, *29*, 23.
(48) (a) Heisel, F.; Miehe, J. A.; Martinho, J. M. G. *Chem. Phys.* **1985**, *98*, 243. (b) Heisel, F.; Miehe, J. A. *Chem. Phys. Lett.* **1986**, *128*, 323.
(49) Su, S.; Simon, J. D. *J. Chem. Phys.* **1988**, *89*, 908.
(50) Lipinski, J.; Chojnacki, H.; Grabowski, Z. R.; Rotkiewicz, K. *Chem. Phys. Lett.* **1980**, *70*, 449.
(51) Majumdar, D.; Sen, R.; Bhattacharyya, K.; Bhattacharyya, S. P. *J. Phys. Chem.* **1991**, *95*, 4324.
(52) Rettig, W.; Koutecky, V. B. *Chem. Phys. Lett.* **1979**, *62*, 115.
(53) Soujanya, T.; Saroja, G.; Samanta, A. *Chem. Phys. Lett.* **1995**, *236*, 503.
(54) Sobolewski, A. L.; Sudholt, W.; Domcke, W. *J. Phys. Chem.* **1998**, *102*, 2716.
(55) Serrano-Andres, L.; Merchan, M.; Roos, B. O.; Lindh, R. *J. Am. Chem. Soc.* **1995**, *117*, 3189.
(56) Lommatzsch, U.; Brutschy, B. *Chem. Phys.* **1998**, *234*, 35.
(57) Sobolewski, A. L.; Domcke, W. *Chem. Phys. Lett.* **1996**, *259*, 119.
(58) Scholes, G. D.; Phillips, D.; Gould, I. R. *Chem. Phys. Lett.* **1997**, *266*, 521.
(59) Kato, S.; Amatatsu, Y. *J. Chem. Phys.* **1990**, *92*, 7241.
(60) Sobolewski, A. L.; Domcke, W. *Chem. Phys. Lett.* **1996**, *250*, 428.
(61) Weisenborn, P. C. M.; Huizer, A. H.; Varma, C. A. G. O. *Chem. Phys.* **1989**, *133*, 437.
(62) Rotkiewicz, K.; Leismann, H.; Rettig, W. *J. Photochem. Photobiol. A: Chem.* **1989**, *49*, 347.
(63) Lardeux, C. D.; Jouvet, C.; Martrenchard, S.; Solgadi, D.; McCombie, J.; Howells, B. D.; Palmer, T. F.; Leitis, A. S.; Monte, C.; Rettig, W.; Zimmermann, P. *Chem. Phys.* **1995**, *191*, 271.
(64) (a) Kobayashi, T.; Futakami, M.; Kajimoto, O. *Chem. Phys. Lett.* **1986**, *130*, 63. (b) Kajimoto, O.; Nayuki, T.; Kobayashi, T. *Chem. Phys. Lett.* **1993**, *209*, 357.
(65) Shang, Q.-Y.; Bernstein, E. R. *J. Chem. Phys.* **1992**, *97*, 60.
(66) Chudoba, C.; Kummrow, A.; Dreyer, J.; Stenger, J.; Nibbering, E. T. J.; Elsaesser, T.; Zachariasse, K. A. *Chem. Phys. Lett.* **1999,** *309*, 357.
(67) Scholes, G. D.; Matousek, P.; Parker, A. W.; Phillips, D.; Towrie, M. *J. Phys. Chem. A* **1998**, *102*, 1431.
(68) Matousek, P.; Parker, A. W.; Phillips, D.; Scholes, G. D.; Toner, W. T.; Towrie, M. *Chem. Phys. Lett.* **1997**, *278*, 56.
(69) Scholes, G. D.; Gould, I. R.; Parker, A. W.; Phillips D. *Chem. Phys.* **1998**, *234*, 21.
(70) Matousek, P.; Towrie, M.; Stanley, A.; Parker, A. W. *J. Appl. Spectrosc. (Engl. Transl.)* **1999**, *53*, 1485.
(71) Towrie, M.; Parker, A. W.; Shaikh, W.; Matousek, P. *Meas. Sci. Technol.* **1998**, *9*, 816.
(72) Matousek, P.; Parker, A. W.; Taday, P. F.; Toner, W. T.; Towrie, M. *Opt. Commun.* **1996**, *127*, 307.
(73) Matousek, P.; Parker, A. W.; Towrie M. Report RAL-95-028; Rutherford Appleton Laboratory, Oxfordshire, UK, 1995.
(74) Herbich, J.; Rotkiewicz, K.; Waluk, J.; Andresen, B.; Thulstrup, E. W. *Chem. Phys.* **1989**, *138*, 105.
(75) Zachariasse, K. A.; Von der Haar, T.; Hebecker, A.; Leinhos, U.; Kuhnle, W. *Pure Appl. Chem.* **1993**, *65*, 1745.
(76) Rotkiewicz, K.; Grabowski, Z. R.; Jasny, J. *Chem. Phys. Lett.* **1975**, *34*, 55.
(77) Rotkiewicz, K.; Grabowski, Z. R.; Krowczynski, A. *J. Lumin.* **1976**, *12/13*, 877.
(78) Kaminska, E. K.; Rotkiewicz, K.; Grabowska, A. *Chem. Phys. Lett.* **1978**, *58*, 379.
(79) Kohler, G.; Grabner, G.; Rotkiewicz, K. *Chem. Phys.* **1993**, *173*, 275.
(80) Gates, P. N.; Steele, D.; Pearce, R. A. R.; Radcliffe, K. *J. Chem. Soc., Perkin Trans. 2* **1972**, 1607.
(81) Schneider, S.; Freunscht, P.; Brehm, G. *J. Raman Spectrosc.* **1997**, *28*, 305.
(82) (a) Tripathi, G. N. R.; Schuler, R. H. *J. Phys. Chem.* **1987**, *91*, 5881. (b) Tripathi, G. N. R.; Schuler, R. H. *J. Chem. Phys.* **1984**, *81*, 113. (c) Tripathi, G. N. R.; Schuler, R. H. *Chem. Phys. Lett.* **1984**, *110*, 542. (d) Tripathi, G. N. R.; Schuler, R. H. *Chem. Phys. Lett.* **1983**, *98*, 594. (e) Tripathi, G. N. R.; Schuler, R. H. *J. Phys. Chem.* **1984**, *88*, 1706.
(83) Hester, R. E.; Williams, K. P. J. *J. Chem. Soc., Faraday Trans. 2* **1981**, *77*, 541.
(84) Katritzky, A. R.; Jones, R. A. *J. Chem. Soc.* **1959**, 3674.
(85) Varsanyi, G. In *Assignments for vibrational spectra of seven hundred benzene derivatives*; Lang, L., Ed.; Adam Hilger: London, 1974; Vol. I.
(86) Brouwer, A. M.; Wilbrandt, R. *J. Phys. Chem.* **1996**, *100*, 9678.
(87) Poizat, O.; Guichard, V. J. *Chem. Phys.* **1989**, *90*, 4697.
(88) Forster, M.; Hester, R. E. *J. Chem. Soc., Faraday Trans. 2* **1981**, *77*, 1535.
(89) Clark, R. J. H.; Hester, R. E. *Time-resolved Spectroscopy*; Wiley: Chichester, 1989; p 166.
(90) Ernstbrunner, E. E.; Girling, R. B.; Grossman W. E. L.; Williams, K. P. J.; Hester, R. E. *J. Raman Spectrosc.* **1981**, *10*, 161.
(91) Heine, A.; Irmer, R. H.; Stalke, D.; Kuhnle, W.; Zachariasse, K. A. *Acta Crystallogr.* **1994**, *B50*, 363.
(92) Finch, A.; Hyams, I. J.; Steele, D. *J. Mol. Spectrosc.* **1965**, *16*, 103.
(93) Hashimoto, M.; Hamaguchi, H. *J. Phys. Chem.* **1995**, *99*, 7875.
(94) Scaiano, J. C. *Handbook of Organic Photochemistry*; CRC Press: Boca Raton, FL, 1989; Vol. II, p 344.
(95) Chattopadhyay, N.; Rommens, J.; Van der Auweraer, M.; De Schryver, F. C. *Chem. Phys. Lett.* **1997**, *264*, 265.
(96) Chandross, E. A. In *The Exciplex;* Gordon, M., Ware, W. R., Eds.; Academic Press: London, 1975; p 187.
(97) Paper in preparation.
(98) Wang, Y.; McAuliffe, M.; Novak, F.; Eisenthal, K. B. *J. Phys. Chem.* **1981**, *85*, 3736.
(99) Nadler, W.; Marcus, R. A. *J. Chem. Phys.* **1987**, *86*, 3906.
(100) Horng, M. L.; Gardecki, J. A.; Papazyan, A.; Maroncelli, M. *J. Phys. Chem.* **1995**, *99*, 17311.
(101) Rossetti, R.; Beck, S. M.; Brus, L. E. *J. Phys. Chem.* **1983**, *87*, 3058.
(102) Anno, T. *J. Chem. Phys.* **1965**, *42*, 932.
(103) Beck, S. M.; Brus, L. E. *J. Am. Chem. Soc.* **1982**, *104*, 4789.
(104) Hester, R. E.; Williams, K. P. J. *J. Chem. Soc., Faraday Trans. 2* **1982**, *78*, 573.
(105) Varsanyi, G.; Kubinyi, M. *J. Mol. Struct.* **1978**, *45*, 107.